

# Permutationless Many-Jet Event Reconstruction with Symmetry Preserving Attention Networks

Michael James Fenton <sup>\*†,1</sup> Alexander Shmakov <sup>\*,2</sup> Ta-Wei Ho,<sup>3</sup> Shih-Chieh Hsu,<sup>4</sup> Daniel Whiteson,<sup>1</sup> and Pierre Baldi<sup>2</sup>

<sup>1</sup>*Department of Physics and Astronomy, University of California Irvine*

<sup>2</sup>*Department of Computer Science, University of California Irvine*

<sup>3</sup>*Department of Physics and Astronomy, National Tsing Hua University, Taiwan*

<sup>4</sup>*Department of Physics and Astronomy, University of Washington*

Top quarks are the most massive particle in the Standard Model and are produced in large numbers at the Large Hadron Collider. As the only quark to decay prior to hadronization, they have a complex detector signature and require special reconstruction techniques. The most common decay mode, the so-called “all-hadronic” channel, results in a 6-jet final state which is particularly difficult to reconstruct in  $pp$  collisions due to the large number of permutations possible. We present a novel approach to this class of problem, based on neural networks using a generalized attention mechanism, that we call Symmetry Preserving Attention Networks (SPA-NET). We train one such network to identify and assign the decay products of each top quark unambiguously and without combinatorial explosion as an example of the power of this technique. This approach significantly outperforms existing state-of-the-art methods, correctly assigning all jets in 93.0% of 6-jet events, 87.8% of events with 7 jets, and 82.6% of events with  $\geq 8$  jets.

## INTRODUCTION

At the Large Hadron Collider (LHC), protons are collided at the highest energy ever produced in the laboratory. Most of these collisions produce events with a high multiplicity of *jets*; collimated sprays of hadronic particles that originate from the strongly-coupled quarks and gluons inside the proton. These “all-jet” final states occur through a number of physical processes, including elastic collisions, production of heavy bosons  $W$ ,  $Z$ , or Higgs, or production of heavy fermions such as the top quark. The copious production presents opportunities for precision measurements and searches for rare processes [1, 2], but also raises particular challenges. Specifically, it is typically difficult to connect an observed jet with its quark origin, and the factorial dependence on the number of jets leads to the so-called “combinatorial explosion”. This is more than a computing challenge, as a large number of incorrect assignments can obscure the crucial physics under study. For example, top quarks most commonly produce three jets each, and gluon radiation, multi-parton interactions, and underlying event remnants may all add additional jets to the final state. Top pair production then has a  $\geq 6$  jet final state, and the biggest obstacle

to extracting physical information from these events is correctly determining which jets originate from each of the parent top quarks.

The top quark is unique in the Standard Model: as the most massive fundamental particle in the theory, it is the only quark to decay before hadronisation can occur. This presents a unique opportunity to study an isolated quark, if its decay products can be correctly identified. Top quarks decay via  $t \rightarrow Wb$ , and pairs are categorized by the decay modes of the pairs of  $W$  boson: dileptonic (9%), single-lepton (45%) or all-jets (46%) [3]. To date, the most precise measurements of top quark properties are typically performed in the single lepton or dilepton channels[4]. The fully hadronic channel, held back by the ambiguous event reconstruction and large all-jet backgrounds, is comparatively under-explored.

In this letter, we propose a novel algorithm for assignment of particle origin to jets, Symmetry Preserving Attention NETwork (SPA-NET). Applying attention networks that naturally reflect the permutation symmetry of the task, SPA-NET significantly outperforms existing state-of-the-art techniques while simultaneously avoiding the combinatorial explosion. In the following, we define the nature of the jet assignment task, describe invariance and attention mechanisms in neural networks, describe the dataset and training, and demonstrate the performance of our technique relative to the state-of-the-art.

\* These authors contributed equally.

† mjfenton@uci.edu

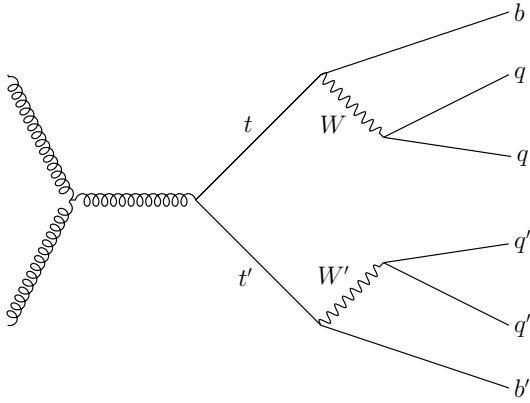


FIG. 1: Diagram of the production of a pair of top quarks,  $t\bar{t}$ , and their decays into  $qq\bar{b}$  and  $\bar{q}'q'b'$ , respectively.

### JET ASSIGNMENT

The jet assignment task, most generally, is the identification of the original quark (or other hadronic particle) which leads to a jet in the detector systems. In a collision which produces  $N$  jets, there are  $N!$  possible assignments. Fortunately, symmetries can help reduce this number.

Top quarks decay via the chain  $t \rightarrow Wb \rightarrow qq\bar{b}$ , disregarding the unobservable quark charge labels. A pair of top quarks,  $t\bar{t}$ , therefore produce six quarks,  $qq\bar{b}q'\bar{b}'$ . This process is shown in Fig. 1. In this context, the jet assignment task is to correctly identify six observed jets with six labels:  $b, \bar{b}', 2 \times q$ , and  $2 \times q'$ . The symmetries between the two tops and between the decay products of the  $W$  bosons reduce this to  $6!/(2 \times 2 \times 2) = 90$  permutations. Despite this simplification, this number of permutations results in an ambiguity that obscures the scientific power of the data, with the many incorrect assignments obscuring information from the single true assignment. It also represents a significant computational penalty when all permutations are evaluated for every event. Sometimes, each permutation must be evaluated *per systematic uncertainty* per event, which is often simply intractable in the large datasets typical in high energy particle physics.

Further complicating the task, roughly 50% of  $t\bar{t}$  events at the LHC are expected to contain at least one additional jet which is not the result of top quark decay, leading to  $7!/(2 \times 2 \times 2) = 630$  or  $8!/(2 \times 2 \times 2 \times 2) = 2520$  permutations<sup>1</sup> in seven- or eight-jet events, respectively.

<sup>1</sup> The additional factor of 2 for eight-jet events is due to the permutation invariance of the extraneous jets.

Even higher jet multiplicity events are also likely, making clear that testing every possible hypothesis is intractable. Nonetheless, the current state-of-the-art techniques for performing jet assignment depend on enumerating and evaluating each permutation to identify the best candidate. The most common technique is a  $\chi^2$ -minimisation method, which scores a permutation based on the consistency of the reconstructed  $W$ -boson masses with known values and similarity of the two reconstructed top quark masses:

$$\chi^2 = \frac{(m_{bqq} - m_{b'q'q'})^2}{\sigma_{\Delta m_{bqq}}^2} + \frac{(m_{qq} - m_W)^2}{\sigma_W^2} + \frac{(m_{q'q'} - m_W)^2}{\sigma_W^2}. \quad (1)$$

After fitting to the relevant distributions in our dataset (described below), we find  $m_W = 81.3$  GeV,  $\sigma_W = 12.3$  GeV and  $\sigma_{\Delta m_{bjj}} = 26.3$  GeV are the expected parameters of  $W$ -boson mass measurements and top-quark mass difference respectively. The  $\chi^2$  is evaluated for every possible permutation of the event, and the permutation with the minimum value of  $\chi^2$  is chosen. This method typically uses additional information that indicates which jets are likely to have come from a  $b$  quark, which reduces the permutations per event, depending on the number of  $b$ -tagged jets. This has been the preferred reconstruction method for ATLAS [5, 6], while CMS have used a similar, though differently defined,  $\chi^2$  method in the past [7].

Another approach that has been considered is the use of Boosted Decision Trees or Deep Neural Networks as permutation classifiers, though these have mostly been employed in the leptonic decay channels where combinatoric explosion is reduced [8, 9], or to reconstruct tops individually [10]. CMS has also used a hybrid  $\chi^2$  and BDT method in the all-jet channel [11].

A more advanced minimisation technique is implemented in the KLFFitter package [12]. Transfer functions are used to represent the detector response in a likelihood function for each permutation, which is minimised to find the best jet assignments. Functionally, this operates similarly to the  $\chi^2$  technique, but has higher CPU demands due to the more complex model. The performance of KLFFitter has previously been shown not to significantly exceed that of the  $\chi^2$  method in the all-jet channel, and therefore is not discussed in this letter.

## INVARIANCE AND ATTENTION IN DEEP NEURAL NETWORKS

Group invariance properties can play an important role in the design of both feed-forward and recursive neural networks [13–15]. For instance, classical convolution neural networks can produce object recognition outputs that are invariant with respect to translations in their two-dimensional inputs, and this invariance property has been generalized to apply to other manifolds and groups [16, 17]. In the problem considered here, the network output should be invariant under permutations of the input jet order. In addition, the output should identify two distinct interchangeable triplets,  $qqb$  and  $q'q'b'$ , each of which include an interchangeable pair,  $qq$  or  $q'q'$ .

Attention mechanisms are essentially gating mechanisms where, for instance, the activities of a set of neurons are multiplied, component-wise, by the activities of another set of neurons. These gating mechanisms allow neural networks to dynamically modulate neural activity in a layer as a function of the activities of other neurons or inputs. Recursive and attention-based neural networks have achieved state-of-the-art performance in natural language processing, for instance in machine translation [18], language understanding [19], and text generation [20]. These models are successful because they allow the network to infer relationships between different elements in a sequence. Attention architectures can be made permutation invariant because rearranging the order of the elements in the input sequence induces the same rearrangement in the attention mechanism. Typically this feature is ignored and sometimes removed with time-dependent embedding, but it can also be leveraged to easily endow the network with permutation symmetry [21], as needed for event reconstruction. Here, we further leverage the permutation invariance present in attention-based methods to efficiently model the symmetries of the top quark pair system. We generalize the ideas present in dot-product attention to allow for a three-way symmetry-preserving attention mechanism which can perform jet assignments into  $qqb$  and  $q'q'b'$  triplets.

## DATASETS

A sample of 30M simulated  $pp \rightarrow t\bar{t}$  events was generated at  $\sqrt{s} = 13$  TeV using MadGraph\_aMC@NLO [22], interfaced to the Pythia8 [23] package for parton showering and hadronisation. Detector response was simulated using Delphes [24] with the ATLAS parameterization. Events are generated at leading order in QCD, with

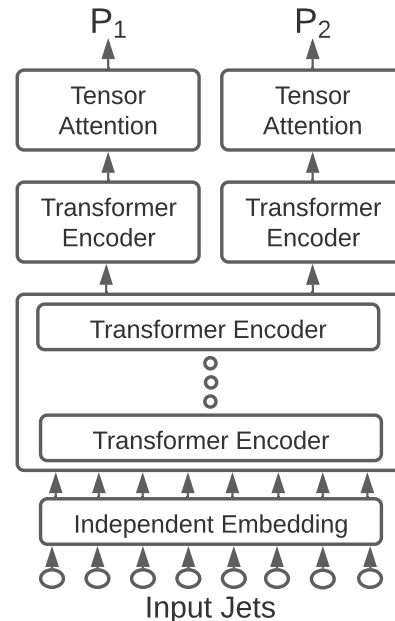


FIG. 2: High Level Structure of SPA-NET.

the top mass  $m_{\text{top}} = 173$  GeV, and the  $W$  boson forced to decay hadronically. Jets are reconstructed using the anti- $k_T$  algorithm [25] with a radius parameters of 0.4, and required to have transverse momentum  $p_T \geq 25$  GeV and absolute pseudo-rapidity  $|\eta| < 2.5$ . Of the generated events, 5 926 407 meet the preselection requirements of  $\geq 6$  jets, with two of these jets further required to be classified as originating from a  $b$  quark. This is performed using a  $p_T$ -dependent efficiency function with 34% efficiency at  $p_T = 25$  GeV and 57% efficiency at  $p_T = 100$  GeV.

The supervised learning technique employed here requires a training sample in which the correct assignments are identified. We define the correct jet assignments by matching them to the simulated truth quarks within an angular distance of  $\Delta R = \sqrt{\Delta\eta^2 + \Delta\phi^2} < 0.4$ . Requiring all six quarks to be unambiguously matched leaves 1,550,210 total events for training, and 386 560 for performance evaluation. This matching requirement has an efficiency of 24% on 6 jet events, 32% on 7 jet events, and 40% on  $\geq 8$  jet events. We also evaluate the performance in events in which only one of the top quarks has all decay products matched. This dataset has a total of 619 818 events, with filter efficiencies of 56%, 52%, and 48% in 6 jet, 7 jet, and  $\geq 8$  jet events respectively.

## SPA-NET ARCHITECTURE

We perform the jet classification with SPA-NET: an attention-based neural network that embeds the symmetries of the problem. Inputs to the network are an unsorted list of jets, each represented by the  $p_T$ ,  $\eta$ ,  $\phi$  and  $M$ , as well as a boolean value representing if the jet was  $b$ -tagged or not. The network, shown in Figure 2, consists of six components: a jet-independent embedding which converts each jet into a  $D$ -dimensional latent space representation; a stack of transformer encoders which learn the relationships between latent vectors; two additional transformer encoders on each branch to prepare the latent vectors for output; and two tensor-attention output layers which produce the top-quark triplet distributions. In this variant, the transformer encoders employ a variant of attention known as multi-head self-attention [18], but they may use any permutation-invariant architecture in general. The initial independent embedding is a simple fully-connected layer which is applied independently to each jet using weight sharing and thus maintaining permutation invariance.

### Symmetry Preserving Tensor Attention

Jet assignment in the context of top quark pairs presents several unique problems for typical classification networks, as a variety of symmetries complicate the output generation and training. Primarily, the physics quantities are invariant under permutation of the  $W$  decay products,  $qq$ . Therefore, the network must not differentiate between predictions which prefer one ordering to the other, and match each  $qq$  pair to the appropriate  $b$ . This naturally creates a triplet relation within the  $qqb$ , with the  $qq$  obeying permutation symmetry. In order to encode this invariance into the network, we develop a generalization of the attention mechanism which can learn  $n$ -way relationships with included symmetries. We call this technique *tensor attention*.

Each tensor attention layer contains a single set of weights  $W \in \mathbb{R}^{D \times D \times D}$ . This tensor is not inherently symmetric: in order to produce an invariant attention weighting, we need to first transform it into an auxiliary weights tensor which conforms to the permutation group of the classification task. We produce  $S \in \mathbb{R}^{D \times D \times D}$  and use it to perform a generalization of weighted dot-product attention on a list of embedded jets  $X \in \mathbb{R}^{N \times D}$ , where  $N$  is the number of jets. Expressed in Einstein summation notation, the tensor attention layer can be described as:

$$S^{nml} = W_{ij}^n W^{mij} W_k^{lk} \quad (2)$$

$$O^{ijk} = X_n^i X_m^j X_l^k S^{nml} \quad (3)$$

The shared indices in the first two terms of Equation 2 guarantee that the first two dimensions of  $S$  will be symmetric. This construction of  $S$  ensures that  $O^{ijk} = O^{jik}$ , enforcing  $qq$  invariance in the output. Afterwards, we perform a 3 dimensional softmax on  $O$  to generate the joint triplet probability distribution

$$P(i, j, k) = \frac{\exp O^{ijk}}{\sum_{i,j,k} \exp O^{ijk}} \quad (4)$$

We produce individual distributions for each of the two top-quarks,  $P_1$  and  $P_2$ , and we extract a single triplet from each  $P$  during evaluation by selecting the peak of these distributions.

An important note here is that the rank of the weights tensor depends only the the hyperparameter  $D$ , and thus, it is possible to include any number of jets in each event. Crucially, unlike all other existing methods, evaluation time per event scales linearly with the number of jets. This removes the crippling limitations of the  $\chi^2$  method, which grows exponentially with the number of jets. In our dataset, the largest jet multiplicity in a single event is  $N = 20$ .

### Training

We train these distributions via cross-entropy between the output probabilities and the true target distribution on the all-jet  $t\bar{t}$  problem, naming the resulting network SPAtTER (SPA-NET for  $t\bar{t}$  Reconstruction). This formulation contains another symmetry which can be exploited. The top quark pairs are invariant with respect to the labels,  $t\bar{t}' = t'\bar{t}$ . We create a symmetric loss function which allows either of the networks two output distributions,  $P_1$  and  $P_2$ , to match either one of the targets  $t$  and  $t'$ , training on the minimum loss between the two permutations. Furthermore, to prevent  $P_1$  and  $P_2$  from collapsing into a single identical distribution, we add an auxiliary symmetric cross-entropy term, mediated by a scalar parameter  $\beta$ , to encourage SPAtTER to separate  $P_1$  and  $P_2$ . The loss  $\mathcal{L}$  is expressed as

$$\mathcal{L} = \mathcal{L}_2(P_1, t, P_2, t') - \beta \mathcal{L}_1(P_1, P_2, P_2, P_1) \quad (5)$$

where

$$\begin{aligned}\mathcal{L}_2(P_1, t, P_2, t') &= \min(\mathcal{L}_1(P_1, t, P_2, t'), \mathcal{L}_1(P_1, t', P_2, t)) \\ \mathcal{L}_1(P_1, T_1, P_2, T_2) &= H(P_1, T_1) + H(P_2, T_2) \\ H(X, Y) &= \sum_{(x, y) \in (X, Y)} -x \log(y)\end{aligned}$$

Nonetheless, this process has a non-zero possibility of classifying the same jet to be part of both triplets. During evaluation, this occurred 5.3% of the time. In these events, we select the assignment from the higher probability  $P$  first, and re-evaluate the other  $P$  to select the best non-contradictory classification.

Another interesting note is that, although we include it as an input feature, SPAT $\bar{t}$ ER does not enforce that the  $b$ -tagged jets are selected in the position of the  $b$ -quarks. This allows the network to correctly predict events in which there are mistagged jets, while still utilising  $b$ -tagging information. In the  $\chi^2$  method, allowing this means  $b$ -tagging information is completely lost, and is only possible by increasing the number of evaluated permutations.

We select optimal hyperparameters for SPAT $\bar{t}$ ER by running a parallel random hyperparameter search using the SHERPA hyperparameter optimization library [26]. We evaluate 500 different sets of hyperparameters before selecting the best-performing model. The optimal found network uses 6 transformer encoder layers, a latent space dimensionality of  $D = 128$ , and the LAMB large batch-size optimizer [27] with a learning rate of  $\alpha = 0.001$  and a batch size of 1024. The final network was trained using four Nvidia Titan V GPUs until convergence at approximately 10 hours.

## PERFORMANCE

To assess the performance of the  $\chi^2$  and SPAT $\bar{t}$ ER techniques, we define two metrics, which can only be evaluated on *identifiable* top quarks, where the correct assignment has been identified as described previously. The first metric is  $\epsilon^{\text{top}}$ , the fraction of identifiable top quarks which have all three jets correctly assigned. This is reported in two event subsets, those where only one top quark is identifiable (as  $\epsilon_1^{\text{top}}$ ), and those where both top quarks are identifiable (as  $\epsilon_2^{\text{top}}$ ). The second metric is  $\epsilon^{\text{event}}$ , the fraction of events with two identifiable top quarks in which both top quarks have all three jets cor-

rectly assigned. Table I shows the  $\epsilon^{\text{top}}$  and  $\epsilon^{\text{event}}$  values for both the  $\chi^2$  and SPAT $\bar{t}$ ER methods.

The baseline  $\chi^2$  method has an  $\epsilon^{\text{event}}$  of 39.8%, while SPAT $\bar{t}$ ER achieves an  $\epsilon^{\text{event}}$  of 86.7%. The  $\chi^2$  technique suffers from a large reduction in performance as jet multiplicity increases, peaking at 63.8% for events with exactly 6 jets and dropping to 25.0% in events with at least 8 jets. In contrast, SPAT $\bar{t}$ ER sees a comparatively small drop in performance with jet multiplicity, at 93.0% in 6 jet events and 82.6% in  $\geq 8$  jet events. We observe a similar trend in the per-top efficiencies; for  $\epsilon_2^{\text{top}}$ , SPAT $\bar{t}$ ER achieves 90.8% inclusively, compared to just 49.1% for the  $\chi^2$  method. These numbers drop to 88.3% and 37.5% respectively in  $\geq 8$  jet events. The performance is lower in events in which only one top is identifiable;  $\epsilon_1^{\text{top}}$  is 45.1% with SPAT $\bar{t}$ ER and 29.3% for the  $\chi^2$  method. We also note that in our evaluation dataset, 8.4% of events in which both tops are identifiable have  $b$ -quarks matched to non- $b$ -tagged jets. These events, which are impossible for the  $\chi^2$  method to correctly reconstruct, are correctly reconstructed by SPAT $\bar{t}$ ER with an efficiency of 63.8%.

TABLE I: Performance of the  $\chi^2$  and SPAT $\bar{t}$ ER assignments assessed by per-event efficiency  $\epsilon^{\text{event}}$  and per-top efficiencies  $\epsilon^{\text{top}}$  (see text for details), reported inclusively and by jet multiplicity  $N_{\text{jets}}$ .

$N_{\text{jets}}$	$\chi^2$ Method			SPAT $\bar{t}$ ER		
	$\epsilon^{\text{event}}$	$\epsilon_2^{\text{top}}$	$\epsilon_1^{\text{top}}$	$\epsilon^{\text{event}}$	$\epsilon_2^{\text{top}}$	$\epsilon_1^{\text{top}}$
6	63.8%	66.8%	31.5%	93.0%	94.7%	48.9%
7	43.2%	52.6%	31.0%	87.8%	91.6%	45.7%
$\geq 8$	25.0%	37.5%	25.4%	82.6%	88.3%	40.8%
<b>Inclusive</b>	<b>39.8%</b>	<b>49.1%</b>	<b>29.3%</b>	<b>86.7%</b>	<b>90.8%</b>	<b>45.1%</b>

We inspect the reconstructed  $W$  and top quark masses using the assignments generated by both methods, to ensure no kinematic bias has been introduced. Figure 3 shows the distributions of  $m_W$  using assignments from both methods, for all events in the preselection region, broken down into three categories: “correct”, “incorrect”, and “unmatched”, corresponding to: cases in which all three top decay products are correctly assigned, cases in which all three top decay products are present in the event but at least one is incorrectly assigned, and cases in which one or more of the top decay products is not identifiable, respectively. The  $\chi^2$  method has a narrower peak around  $m_W$  than SPAT $\bar{t}$ ER, though much of this shape comes from the incorrect and unmatched events. Figure 4 shows the  $m_{\text{top}}$  distributions for the same three categories of event. In this distribution, SPAT $\bar{t}$ ER has the

more peaked distribution, with comparable shapes in the incorrect and unmatched events. Figure 5 shows the distributions of  $m_W$  and  $m_{\text{top}}$  for truth matched jets, SPAT $\bar{t}$ ER predictions, and  $\chi^2$  predictions. Figure 5 shows that the SPAT $\bar{t}$ ER predictions are much closer to the truth distributions than the  $\chi^2$ , as expected from the reconstruction efficiencies in Table I. The  $\chi^2$  predicts a larger tail in  $m_{\text{top}}$  than the truth or SPAT $\bar{t}$ ER predictions, while the  $m_W$  distribution that even more sharply peaked than the truth. Both of these effects are expected - the incorrect triplet predictions will typically overestimate  $m_{\text{top}}$ , while the explicit use of  $m_W$  in Equation 1 explains the narrower peak.

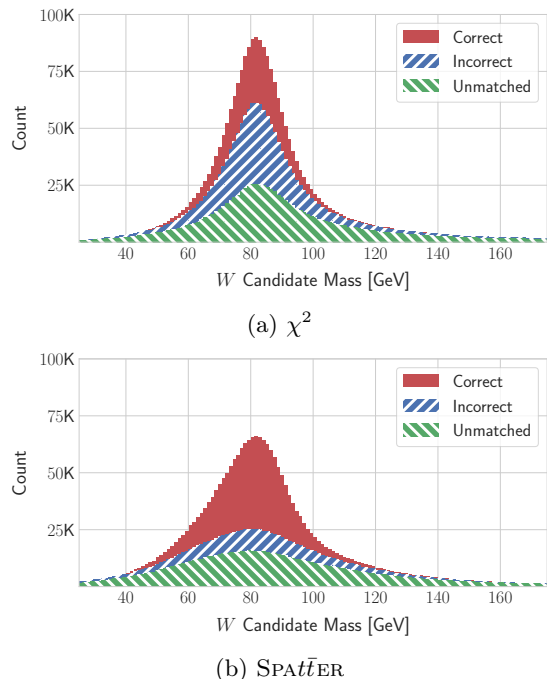


FIG. 3: Stacked distributions of reconstructed  $m_W$  using assignments generated (a) by the  $\chi^2$  method, and (b) by SPAT $\bar{t}$ ER. The solid red shows the distributions for events in which the entire triplet of jets is correctly assigned, the dashed blue shows the distribution for events with at least one jet that is incorrectly assigned, and the dashed green shows the distribution in events where the correct assignment is not identifiable.

A final important performance metric is the computation time per event in each method. The time required to evaluate the  $\chi^2$  method scales approximately factorially with the number of jets in the event, and this often leads to analyses setting a maximum number of jets to consider, degrading the performance for purely CPU-time reasons. On the author’s laptop, a 2019 Dell XPS 13 with an Intel Core i7-1065G7 CPU @ 1.30GHz, SPAT $\bar{t}$ ER

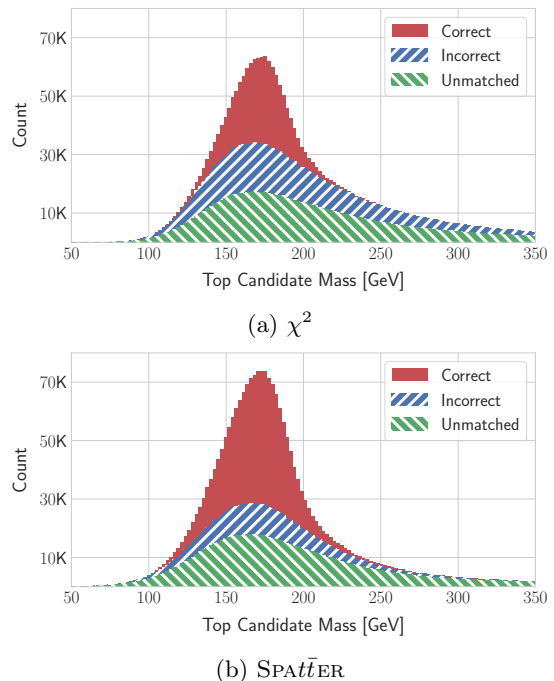


FIG. 4: Stacked distributions of reconstructed  $m_{\text{top}}$  using assignments generated (a) by the  $\chi^2$  method, and (b) by SPAT $\bar{t}$ ER. The solid red shows the distributions for events in which the entire triplet of jets is correctly assigned, the dashed blue shows the distribution for events with at least one jet that is incorrectly assigned, and the dashed green shows the distribution in events where the correct assignment is not identifiable.

took an average of 4.4 ms to evaluate per event, with no dependence on jet multiplicity<sup>2</sup>. In contrast, the  $\chi^2$  took an average of 20 ms in 6-jet events, 48 ms in 7-jet events, and 369 ms in  $\geq 8$ -jet events.

## CONCLUSIONS

SPA-NET’s have inherent permutation symmetries which make them very well suited to the task of jet assignment, where the permutations otherwise lead to a combinatoric explosion which increases computation time and dilutes the scientific value of the data. Our network SPAT $\bar{t}$ ER demonstrates superior performance on this task, which is essential to unlocking the power of the important

<sup>2</sup> In principle, evaluation time is linearly dependent on  $N_{\text{jets}}$ ; but, for simplicity, we pad all of the events to the maximum of 20 jets. The speed could be improved through intelligent batching of events by jet multiplicity, though this is not performed here.

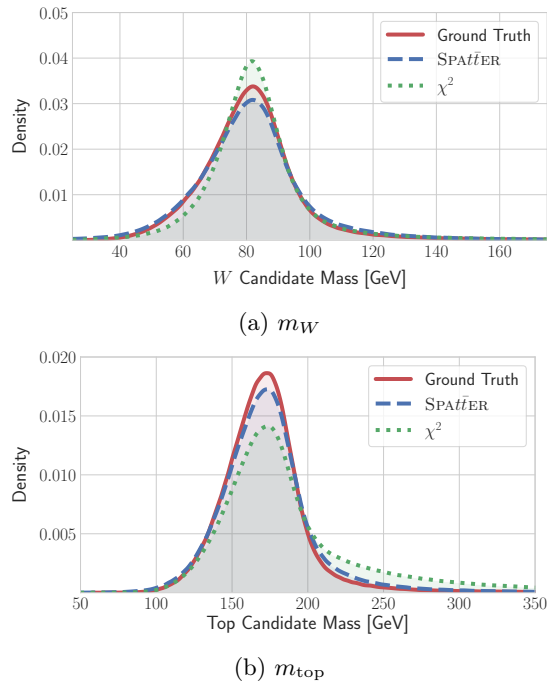


FIG. 5: Comparison of (a)  $m_W$ , and (b)  $m_{\text{top}}$ , for the truth matched jets (solid red), the  $\chi^2$  assignments (dotted green), and the SPATtER assignments (dashed blue). A Gaussian KDE has been applied to data shown in Figs. 3 and 4.

multi-jet dataset at the LHC. The adoption of our technique by the large experimental collaborations ATLAS and CMS will lead to significantly improved precision of analyses, such as measurements of top mass or differential cross-section, in the all-jet  $t\bar{t}$  final state by improving the fraction of events that are well reconstructed from 39.8% using existing methods to 86.7% using our new technique. This paradigm shift in the all-jet channel will allow greatly enhanced sensitivity in high jet multiplicity events and many new analyses viable in this final state.

This letter describes just one of many possible applications of SPA-NET’s to event reconstruction in high energy particle physics. Future work may include extending these techniques to alternative all-jet final states, to other  $t\bar{t}$  decay modes, or many other classes of problem. Though not studied here, the output of SPATtER may also be used in additional ways, such as setting a minimum reconstruction quality requirement that will act to suppress backgrounds, analogously to how the  $\chi^2$  is used in [6]. Additional input information, such as jet substructure [28] or (pseudo-)continuous  $b$ -tagging [29], may also improve performance. Another future avenue of interest would be to allow 5 jet events - in which one of the de-

cay products is extremely soft, or one of the  $W$  bosons is highly boosted - to be matched accordingly, increasing the number of events with a possible “correct” solution.

This letter contributes to a family of work which help endow machine learning methods with problem specific invariances. We have presented an efficient linear-time approach for tackling classification tasks where the targets must obey a set of permutation symmetries. Such symmetries underlie the mathematical foundation of the Standard Model, but they may be found in many other common classification tasks. Graph matching [30] and hierarchical clustering algorithms typically require a combinatorial ranking of possible pairings in order to select the most likely candidates. Well trained deep neural networks can replace these ranking algorithms, and avoid these combinatorial explosions, by effectively estimating symmetry-aware pair-wise similarities. Symmetries can also be used to creating smaller, more focused network models that reduce the amount of data necessary for training [31]. Understanding and exploiting the invariances present in nearly every modeling task is vital for effective learning.

## ACKNOWLEDGEMENTS

MF would like to thank Megan Remillard for language editing assistance. DW and MF are supported by the U.S. Department of Energy (DOE), Office of Science under Grant No. DE-SC0009920. S.-C. Hsu is supported by the U.S. Department of Energy, Office of Science, Office of Early Career Research Program under Award number DE-SC0015971. The work of T.-W.H. was supported by the Taiwan MoST with the grant number MOST-107-2112- M-007-029-MY3. The work of AS and PB in part supported by grants NSF NRT 1633631 and ARO 76649-CS to PB.

- 
- [1] ATLAS Collaboration. Search for resonances decaying into top-quark pairs using fully hadronic decays in  $pp$  collisions with ATLAS at  $\sqrt{s} = 7$  TeV. *JHEP*, 01:116, 2013.
  - [2] CMS Collaboration. Search for vector-like T quarks decaying to top quarks and Higgs bosons in the all-hadronic channel using jet substructure. *JHEP*, 06:080, 2015.
  - [3] M. Tanabashi et al. Review of Particle Physics. *Phys. Rev. D*, 98(3):030001, 2018.
  - [4] CMS D0 ATLAS, CDF. First combination of Tevatron and LHC measurements of the top-quark mass. 3 2014.

- [5] ATLAS Collaboration. Top-quark mass measurement in the all-hadronic  $t\bar{t}$  decay channel at  $\sqrt{s} = 8$  TeV with the ATLAS detector. *JHEP*, 09:118, 2017.
- [6] ATLAS Collaboration. Measurements of top-quark pair single- and double-differential cross-sections in the all-hadronic channel in  $pp$  collisions at  $\sqrt{s} = 13$  TeV using the ATLAS detector. 6 2020.
- [7] CMS Collaboration. Measurement of the top quark mass in the all-jets final state at  $\sqrt{s} = 13$  TeV and combination with the lepton+jets channel. *Eur. Phys. J. C*, 79(4):313, 2019.
- [8] J. Erdmann, T. Kallage, K. Kröninger, and O. Nackenhorst. From the bottom to the top—reconstruction of  $t\bar{t}$  events with deep learning. *Journal of Instrumentation*, 14(11):P11015–P11015, Nov 2019.
- [9] ATLAS Collaboration. Search for the standard model Higgs boson produced in association with top quarks and decaying into a  $b\bar{b}$  pair in  $pp$  collisions at  $\sqrt{s} = 13$  TeV with the ATLAS detector. *Phys. Rev. D*, 97(7):072016, 2018.
- [10] ATLAS Collaboration.  $CP$  Properties of Higgs Boson Interactions with Top Quarks in the  $t\bar{t}H$  and  $tH$  Processes Using  $H \rightarrow \gamma\gamma$  with the ATLAS Detector. *Phys. Rev. Lett.*, 125(6):061802, 2020.
- [11] CMS Collaboration. Measurement of the  $t\bar{t}b\bar{b}$  production cross section in the all-jet final state in  $pp$  collisions at  $\sqrt{s} = 13$  TeV. *Phys. Lett. B*, 803:135285, 2020.
- [12] Johannes Erdmann, Stefan Guindon, Kevin Kroeninger, Boris Lemmer, Olaf Nackenhorst, Arnulf Quadt, and Philipp Stolte. A likelihood-based reconstruction algorithm for top-quark pairs and the KLFitter framework. *Nucl. Instrum. Meth. A*, 748:18–25, 2014.
- [13] P. Baldi. The inner and outer approaches for the design of recursive neural networks architectures. *Data Mining and Knowledge Discovery*, DOI: 10.1007/s10618-017-0531-0:1–13, 2017. Available at: <http://link.springer.com/article/10.1007/s10618-017-0531-0>.
- [14] P. Baldi. *Deep Learning in Science: Theory, Algorithms, and Applications*. Cambridge University Press, Cambridge, UK, 2020. In press.
- [15] Forest Agostinelli, Stephen McAleer, Alexander Shmakov, and Pierre Baldi. Solving the rubik’s cube with deep reinforcement learning and search. *Nature Machine Intelligence*, 1(8):356–363, July 2019.
- [16] Taco Cohen, Maurice Weiler, Berkay Kicanaoglu, and Max Welling. Gauge equivariant convolutional networks and the icosahedral CNN. volume 97 of *Proceedings of Machine Learning Research*, pages 1321–1330, Long Beach, California, USA, 09–15 Jun 2019. PMLR.
- [17] Taco Cohen and Max Welling. Group equivariant convolutional networks. volume 48 of *Proceedings of Machine Learning Research*, pages 2990–2999, New York, New York, USA, 20–22 Jun 2016. PMLR.
- [18] Ashish Vaswani, Noam Shazeer, Niki Parmar, Jakob Uszkoreit, Llion Jones, Aidan N Gomez, Łukasz Kaiser, and Illia Polosukhin. Attention is all you need. In I. Guyon, U. V. Luxburg, S. Bengio, H. Wallach, R. Fergus, S. Vishwanathan, and R. Garnett, editors, *Advances in Neural Information Processing Systems 30*, pages 5998–6008. Curran Associates, Inc., 2017.
- [19] Jacob Devlin, Ming-Wei Chang, Kenton Lee, and Kristina Toutanova. BERT: Pre-training of deep bidirectional transformers for language understanding. In *Proceedings of the 2019 Conference of the North American Chapter of the Association for Computational Linguistics: Human Language Technologies, Volume 1 (Long and Short Papers)*, pages 4171–4186, Minneapolis, Minnesota, June 2019. Association for Computational Linguistics.
- [20] Alec Radford, Jeff Wu, Rewon Child, David Luan, Dario Amodei, and Ilya Sutskever. Language models are unsupervised multitask learners. 2019.
- [21] Juho Lee, Yoonho Lee, Jungtaek Kim, Adam Kosiorek, Seungjin Choi, and Yee Whye Teh. Set transformer: A framework for attention-based permutation-invariant neural networks. volume 97 of *Proceedings of Machine Learning Research*, pages 3744–3753, Long Beach, California, USA, 09–15 Jun 2019. PMLR.
- [22] J. Alwall, R. Frederix, S. Frixione, V. Hirschi, F. Maltoni, O. Mattelaer, H. S. Shao, T. Stelzer, P. Torrielli, and M. Zaro. The automated computation of tree-level and next-to-leading order differential cross sections, and their matching to parton shower simulations. *JHEP*, 07:079, 2014.
- [23] Torbjörn Sjöstrand, Stefan Ask, Jesper R. Christiansen, Richard Corke, Nishita Desai, Philip Ilten, Stephen Mrenna, Stefan Prestel, Christine O. Rasmussen, and Peter Z. Skands. An introduction to PYTHIA 8.2. *Comput. Phys. Commun.*, 191:159–177, 2015.
- [24] J. de Favereau, C. Delaere, P. Demin, A. Giammanco, V. Lemaitre, A. Mertens, and M. Selvaggi. DELPHES 3, A modular framework for fast simulation of a generic collider experiment. *JHEP*, 02:057, 2014.
- [25] Matteo Cacciari, Gavin P. Salam, and Gregory Soyez. The anti- $k_t$  jet clustering algorithm. *JHEP*, 04:063, 2008.
- [26] Lars Hertel, Julian Collado, Peter Sadowski, Jordan Ott, and Pierre Baldi. Sherpa: Robust hyperparameter optimization for machine learning. *SoftwareX*. In press.
- [27] Yang You, Jing Li, Sashank Reddi, Jonathan Hseu, Sanjiv Kumar, Srinadh Bhojanapalli, Xiaodan Song, James Demmel, Kurt Keutzer, and Cho-Jui Hsieh. Large batch optimization for deep learning: Training bert in 76 minutes. In *International Conference on Learning Representations*, 2020.
- [28] Andrew J. Larkoski, Ian Moulton, and Benjamin Nachman. Jet Substructure at the Large Hadron Collider: A Review of Recent Advances in Theory and Machine Learning. *Phys. Rept.*, 841:1–63, 2020.
- [29] ATLAS Collaboration. ATLAS b-jet identification performance and efficiency measurement with  $t\bar{t}$  events in  $pp$  collisions at  $\sqrt{s} = 13$  TeV. *Eur. Phys. J. C*, 79(11):970, 2019.
- [30] Tibério S. Caetano, Julian J. McAuley, Li Cheng, Quoc V. Le, and Alexander J. Smola. Learning graph matching. *CoRR*, abs/0806.2890, 2008.



- [31] Benjamin Bloem-Reddy and Yee Whye Teh. Probabilistic symmetries and invariant neural networks. *Journal of Machine Learning Research*, 21(90), 2020.